

Received February 6, 2022, accepted February 26, 2022, date of publication March 2, 2022, date of current version March 15, 2022.

Digital Object Identifier 10.1109/ACCESS.2022.3156265

# Optimizing the Light Source Layout of the Indoor Visible Light Communication System

CHE LIU<sup>1</sup>, YANFENG TANG, WENJIE YAN<sup>1</sup>, AND YAFANG BAI<sup>1</sup>

School of Electronics and Communication Engineering, Changchun University of Science and Technology, Changchun, Jilin 130022, China

Corresponding author: Yanfeng Tang (tangyanfeng@126.com)

**ABSTRACT** Aiming at the problem of uneven illuminance distribution in traditional indoor optical communication systems, this paper proposes a square + elliptical layout, using simulated annealing particle swarm algorithm to optimize the spacing of LED light sources, and optimize the uniformity of system illuminance and signal-to-noise ratio. The simulation results show that the optimized square + elliptical layout illumination ranges from 359.25 lx to 451.05 lx, and the mean square error reaches 12.66 lx. Signal noise ratio is between 18.54 dB and 20.75 dB, and the mean square error is 0.39 dB. Compared with the traditional square and elliptical layout, the illumination performance and communication performance are improved clearly, which provides a new reference scheme for indoor light source layout.

**INDEX TERMS** Visible light communication system, illuminance, signal-to-noise ratio, light source layout.

## I. INTRODUCTION

Single With the rapid development of information technology in recent years, the demand for wireless communication is gradually increasing. As a new communication method, visible light communication technology has gradually replaced the traditional wireless communication technology, visible light communication technology has gradually replaced traditional wireless communication technology [1], [2]. Compared with traditional radio frequency communication technology, visible light communication has the characteristics of high modulation bandwidth, strong confidentiality, and high signal-to-noise ratio. In order to realize the application of indoor visible light communication [3]–[5]. In order to realize the application of indoor visible light communication, it is necessary to arrange the light source. Reasonable light source layout can maximize the performance of the communication system [6].

Due to the huge development prospects of visible light communication technology, it has become one of the current research hotspots. Komine and Nakagawa [7] obtained the illuminance distribution and signal-to-noise ratio distribution of the traditional square layout by simulating a  $5\text{ m} \times 5\text{ m} \times 3\text{ m}$  room, and discussed the effects of inter-symbol interference and reflection. Zhao and Peng [8] proposed a  $4 + 1$  layout based on the traditional layout, and optimized the original

layout while considering the uniformity of illumination and communication performance at the same time. Liu *et al.* [9] optimized the square layout using multiple population genetic algorithms, and the experimental results showed that the optimized layout power distribution is more even. Guo and Tian [10] proposed an LED array with light strips, by searching for the optimal spacing between the light strips and the optimal spacing of the LED array, to achieve the optimization of the light source layout.

At present, most of the research focuses on finding the optimal distance between LEDs. Few people optimize the layout of light sources by controlling the number of LEDs. This paper proposes a square + elliptical layout method through adaptive simulated annealing particles. The group algorithm seeks the optimal distance between LEDs, and at the same time finds the optimal number of LEDs in the elliptical layout, so as to optimize indoor lighting performance and communication performance while reducing system power consumption.

## II. INDOOR VISIBLE LIGHT COMMUNICATION SYSTEM MODEL

Constructing a  $6\text{ m} \times 5\text{ m} \times 3\text{ m}$  rectangular room model as shown in Figure 1, the receiving plane is  $2.15\text{ m}$  away from the roof. The coordinate system is established with the center of the bottom of the rectangle as the origin. The  $x$ -axis and  $y$ -axis are parallel to the two bottom edges of the room

The associate editor coordinating the review of this manuscript and approving it for publication was Meng-Lin Ku<sup>1</sup>.

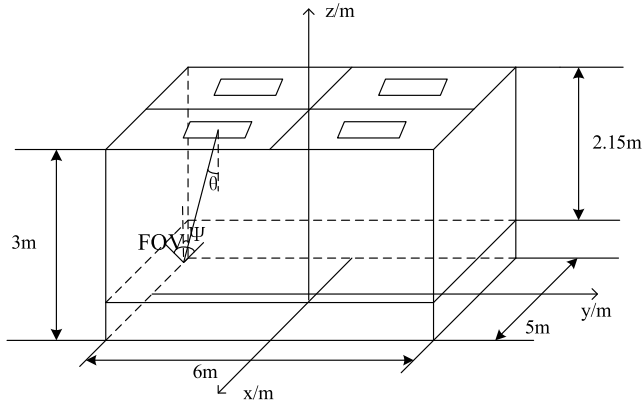


FIGURE 1. Optical communication system model.

respectively, and the  $z$  - axis is perpendicular to the ground. The light source is placed at the top of the room.

Indoor optical communication links are divided into line-of-sight links(LOS) and non - line - of - sight links(NLOS). Studies show that in the receiving plane, direct received power accounts for 93.03% of the total received power, and reflected light for the first time accounts for 5.53% of the total received power. The proportion of two or more reflections in the total received power is very small, so this paper only studies the impulse response of direct and the first time reflection. The emission model of the ideal LED light source follows the Lambert distribution model, and the radiation distribution function of the light source can be expressed as

$$R_0(\theta) = \frac{m + 1}{2\pi} \cos^m(\theta). \quad (1)$$

$\theta$  is radiation angle of LED light source, and  $m$  is the number of radiation patterns of the light source.

For the LOS link, the illuminance formula of the receiver plane can be expressed as

$$E_{LOS} = \frac{I_0 \cos^m(\theta)}{D^2} \cos(\Psi). \quad (2)$$

$I_0$  is the intensity of light when irradiated vertically,  $\theta$  is LED radiation angle,  $\Psi$  is the receiving angle of receiver, and  $D$  is the distance between the receiver and the light source.

For NLOS links, this article proposes that the four walls of the room are considered four mirrors in this article. The four dotted rectangles as shown in Figure 2 are the images of the original rectangle reflected by four mirrors. The illuminance of the source array in the newly generated rectangle multiplied by the reflectance of the original rectangular receiver is equal to the primary reflectance of the original source array.

The illuminance of the NLOS can be expressed by the following formula.

$$E_{NLOS} = \sum_{i=1}^4 0.8 \frac{I_0 \cos^m(\theta_i)}{D_i^2} \cos(\Psi_i). \quad (3)$$

In the above formula, 0.8 is the reflectivity of the wall, so the total illuminance of the receiver plane can be

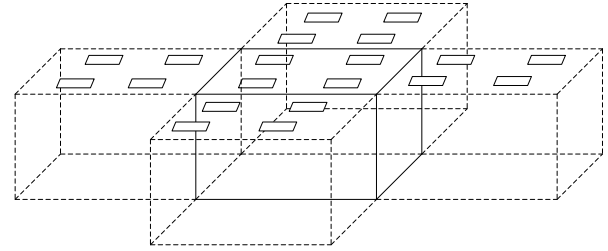


FIGURE 2. Mirror image of the light source once reflected.

expressed as

$$E = E_{LOS} + E_{NLOS}. \quad (4)$$

LED light source is transmitted to the receiving plane through the channel, and the DC gain of the channel can be expressed as

$$H(0) = \begin{cases} \frac{A_{rx} R_0(\theta)}{D^2} \cos(\psi) T_s(\psi) g_s(\psi), & 0 < \psi < \psi_c \\ 0, & \psi > \psi_c. \end{cases} \quad (5)$$

$A_{rx}$  is the area of the receiving detector,  $R_0(\theta)$  is LED radiation distribution function,  $D$  is the distance between the detector and the light source,  $T_s(\psi)$  is the optical filter gain,  $g_s(\psi)$  is the concentrator gain, and  $\psi$  is the field of view of the receiver.

The signal power received at a certain point on the receiving plane is equal to the sum of the received power of all LED arrays at that point, which can be expressed as

$$P_t = \sum_{i=0}^n P_{ti} H_i(0). \quad (6)$$

$P_{ti}$  and  $H_i(0)$  represent the transmit power of the  $i$ -th LED and the DC gain of the channel respectively, and  $n$  is the number of LEDs.

### III. LIGHT SOURCE LAYOUT AND OPTIMIZATION

#### A. ALGORITHM OPTIMIZATION

The advantage of the PSO algorithm lies in its fast convergence speed and simple algorithm [11]. However, PSO algorithm also has the problem of weak search ability and easy to fall into local optimal solution. In order to solve this problem [12]–[14], this paper improves the algorithm from two aspects.

#### 1) THE IMPROVEMENT OF INERTIA FACTOR AND LEARNING FACTOR

##### $\alpha$ : INERTIA FACTOR

The inertia factor affects the global search ability and local search ability of the algorithm. As the iteration progresses, the particles need stronger local search ability, so the inertia factor should be gradually reduced. This article proposes an improved method for the inertia factor as

$$w(k) = w_{max} - w_{min} \sqrt{\frac{k}{T_{max}}}. \quad (7)$$

In the above formula,  $w(k)$  is the improved inertia factor,  $w_{max}$  is the maximum inertia factor,  $w_{min}$  is the minimum inertia factor,  $k$  is the current iteration number,  $T_{max}$  is the maximum iteration number.  $w_{max}$  and  $w_{min}$  take values 0.4 and 0.9 respectively, and  $T_{max}$  takes value 200.

**b: LEARNING FACTOR**

The learning factor,  $c_1$  and  $c_2$ , represents the individual learning ability and the group learning ability of the particle, as the iteration progresses, the particles need to gradually enhance the group learning ability and reduce the individual learning ability. On this basis, this article improves the learning factor.

$$c_1(k) = c_1 - c_1 \sqrt{\frac{k}{T_{max}}} \tag{8}$$

$$c_2(k) = c_2 + c_2 \sqrt{\frac{k}{T_{max}}} \tag{9}$$

In the above formula,  $c_1(k)$  and  $c_2(k)$  represent the improved individual learning factor and group learning factor respectively.  $c_1$  and  $c_2$  take values 0.4 and 0.9 respectively, are the value of the learning factor at the beginning of the algorithm iteration.

**2) SIMULATED ANNEALING ALGORITHM**

This paper incorporates the annealing process in the simulated annealing algorithm into the particle swarm algorithm. When the initial temperature of the algorithm is high, simulated annealing particle swarm optimization makes population examples have larger probability to accept the optimal solution, so as to jump out of local optimal solution [15]. Specific algorithm process is shown in the Figure 3.

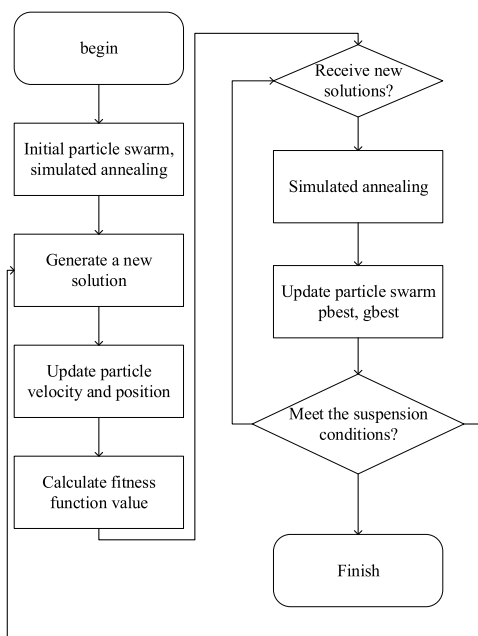


**FIGURE 3. Flow chart of simulated annealing particle swarm algorithm.**

**B. LIGHT SOURCE LAYOUT OPTIMIZATION**

The traditional square layout and elliptical layout are shown in the follow figures and all light sources are distributed on the roof with a height of 3 meters. The square layout in Figure 4(a) consists of four  $9 \times 9$  LED arrays, where  $x_1$  is the distance between the edge of the LED array and the x-axis,  $y_1$  is the distance between the edge of the LED array and the y-axis,  $d$  is the distance between the LEDs in the array. The elliptical layout in Figure 4(b) consists of 324 LED arrays evenly distributed on the ellipse, where  $x_2$  is the length of the long axis of the ellipse and  $y_2$  is the length of the short axis of the ellipse.

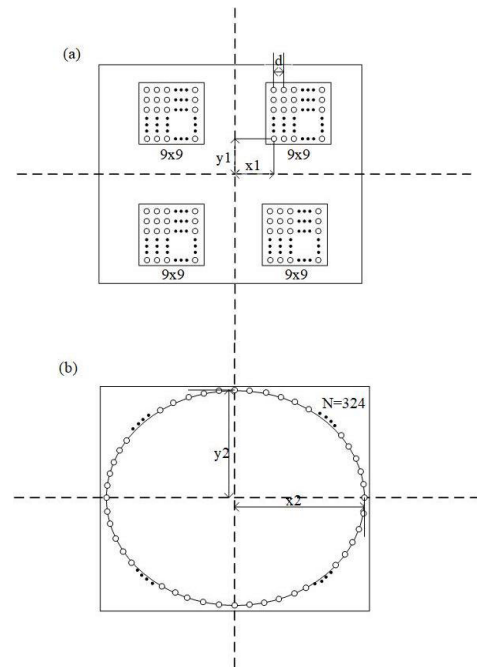


**FIGURE 4. (a) Square layout map (b) Elliptical layout map.**

Use the algorithm mentioned above to optimize the square  $x_1$ ,  $x_2$ ,  $d$  and the ellipse  $x_2$ ,  $y_2$ , and change the indoor light source layout by changing the overall shape of the square and ellipse, thereby optimizing the indoor illumination distribution.

Figure 5 shows the illuminance for square and elliptical layouts picture. It can be seen from the figure that the mean square deviation of the illuminance of the square layout is 31.32 lx, and the uniformity is 77.70%. The mean square deviation of the illuminance of the elliptical layout is 35.46 lx, and the uniformity is 75.21%.

As can be seen from Figure 5 although the traditional square layout and elliptical layout can meet the basic requirements of indoor communication and identification, there are still problems such as uneven illumination. In order to solve these problem, this paper proposes a square + elliptical layout. As shown in Figure 5, the model consists of four  $7 \times 7$  square arrays and  $N$  equally spaced elliptical arrays.

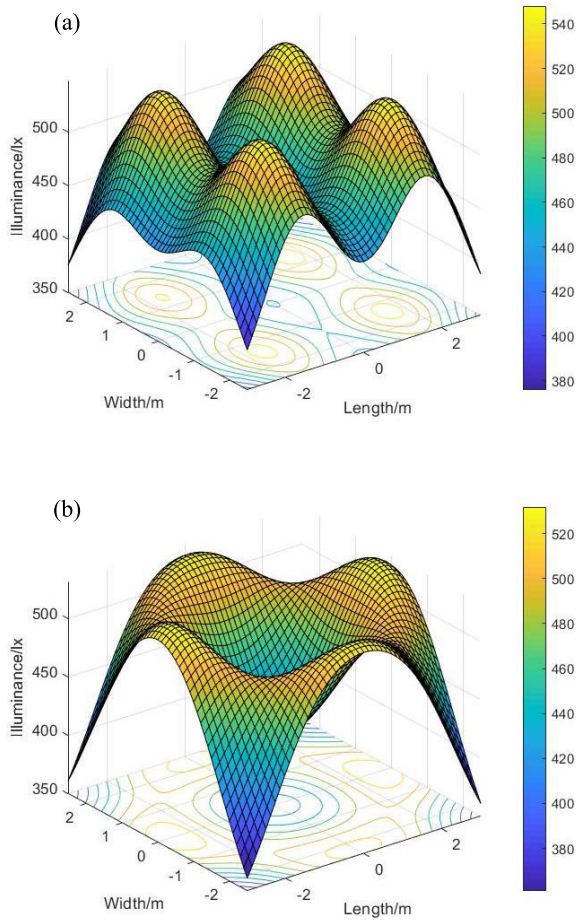


FIGURE 5. (a) Illumination distribution of square layout (b) Illumination distribution of elliptical layout.

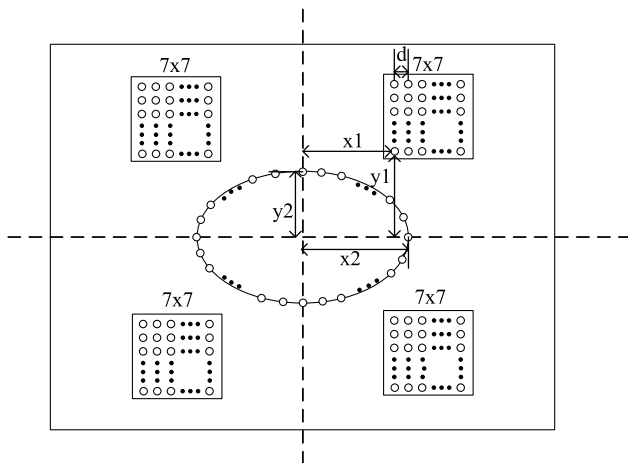


FIGURE 6. Square + elliptical layout.

In the Figure 6,  $x_1, x_2, y_1, y_2$  and  $d$  are the targets to be optimized. In order to ensure the uniformity of the system's illuminance and the reliability of communication, this paper chooses the combination of the mean square error of

illuminance and the mean value of the signal-to-noise ratio  $f(x_1, x_2, y_1, y_2, d)$  as the optimal function. The function can be expressed as

$$f(x_1, x_2, y_1, y_2, d) = f_1 + \alpha \frac{1}{f_2} \tag{10}$$

where  $f_1$  is the mean square error of illuminance, and  $f_2$  is the mean value of the signal-to-noise ratio of the receiving plane. The value of  $\alpha$  in this article is 10.

In order to study the influence of the number of LEDs in the ellipse on the performance of the system, this paper studies the illuminance and signal-to-noise ratio of the system when  $N$  is equal to 60-120.

According to the data in Table 1 and Table 2, it can be indicated that as the number of LEDs in the ellipse increases, the maximum, minimum, average and mean square deviation of

TABLE 1. Illuminance parameters when N takes different values.

	Maximum /lx	Minimum /lx	Average /lx	Mean square error /lx
N = 60	411.85	315.24	379.36	14.19
N = 70	425.02	360.34	393.53	13.43
N = 80	438.03	344.20	407.85	12.88
N = 90	451.05	359.25	421.95	12.66
N = 100	465.42	374.26	436.10	12.78
N = 110	480.27	388.38	450.55	12.85
N = 120	494.92	402.63	464.90	12.99

TABLE 2. SNR parameters when N takes different values.

	Maximum /dB	Minimum /dB	Average /dB	Mean square error /dB
N = 60	19.97	17.32	18.92	0.47
N = 70	20.23	17.76	19.24	0.43
N = 80	20.49	18.14	19.55	0.40
N = 90	20.75	18.54	19.84	0.39
N = 100	21.02	18.92	20.13	0.39
N = 110	21.30	19.25	20.41	0.37
N = 120	21.56	19.58	20.68	0.37

the system’s illuminance and signal-to-noise ratio gradually increases.

Figure 7 illustrates the relationship between the number of  $N$  and the objective function in the elliptical layout. It can be seen from the figure that as the number of LEDs in the elliptical layout increases, the value of the objective function first gradually decreases and then gradually grows until the objective function reaches its minimum value when  $N$  takes 90. So the value of  $N$  in this article is considered to be 90.

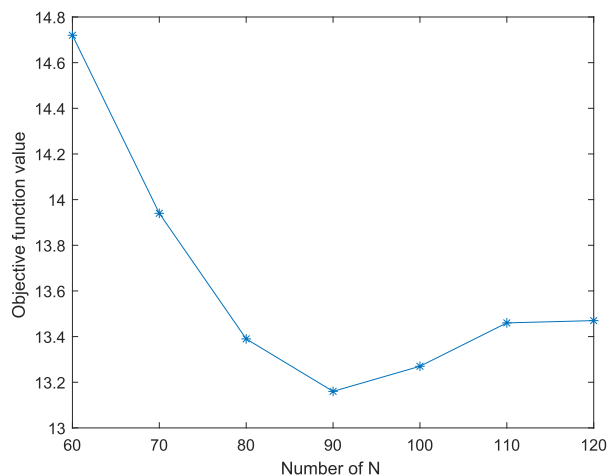


FIGURE 7. The relationship between the number of  $N$  and the objective function.

IV. SIMULATION EXPERIMENT AND DATA ANALYSIS

The light source luminescence mode used in this article is Lambertian luminescence mode, and the specific simulation parameters are listed in Table 3.

This article compares the two common layouts of square and elliptical with the layout proposed in this article. Since the system performance analysis of the indoor visible light communication system should consider not only the communication performance, but also the lighting performance of the system, this article analyzes the system under different layouts from the perspective of lighting and communication.

A. LIGHTING PERFORMANCE ANALYSIS

The experimental results show that the maximum illuminance of the square + elliptical layout is 451.05 lx, the minimum is 359.25 lx, the mean square error is 12.66 lx, and the uniformity is 85.14%.

The above-mentioned experimental data shows that the illuminance range of whether it is square, elliptical or square + elliptical layout ranges from 300 lx to 1500 lx [16], meeting the internationally regulated indoor lighting standards. But compared with the traditional square and elliptical layout, the layout model proposed in this paper reduces the dynamic range of illuminance and improves the uniformity of illuminance.

TABLE 3. Simulation experiment parameters.

Parameter	Value
Room size	6 m × 5 m × 3 m
Single led bulb power	2.0 w
Center luminous intensity	21.5 cd
Photodiode responsivity	0.53 A/W
Field of view at receiver	70°
Refractive index of concentrator n	2
Half power angle	70°
Gain of an optical filter	1.0
Background noise current	0.62 mA
Equivalent noise bandwidth	200 MHZ
Load resistance	10KΩ
Reflectivity of walls	0.8
Detector physical area of a photodiode A	1cm <sup>2</sup>

In order to verify the authenticity of the Matlab simulation results, this paper uses the Dialux software to analyze the above three the light source layout method which is simulated to obtain the real distribution of room illumination.

Figure 8 shows the iso-illuminance diagram of the receiving plane 0.75 m away from the ground under the three light source layouts. It can be seen from the figure that the illuminance of the receiving plane is basically the same as the simulation result of Matlab.

B. COMMUNICATION PERFORMANCE ANALYSIS

Figure 9(a) is a traditional square layout receiving plane signal-to-noise ratio distribution. The signal-to-noise ratio ranges from 18.64 dB to 22.59 dB, and the mean square error is 0.80 dB. Figure 9(b) is the traditional elliptical layout receiving plane SNR distribution. The SNR ranges from 18.04 dB to 22.23 dB, and the mean square error is 0.93 dB.

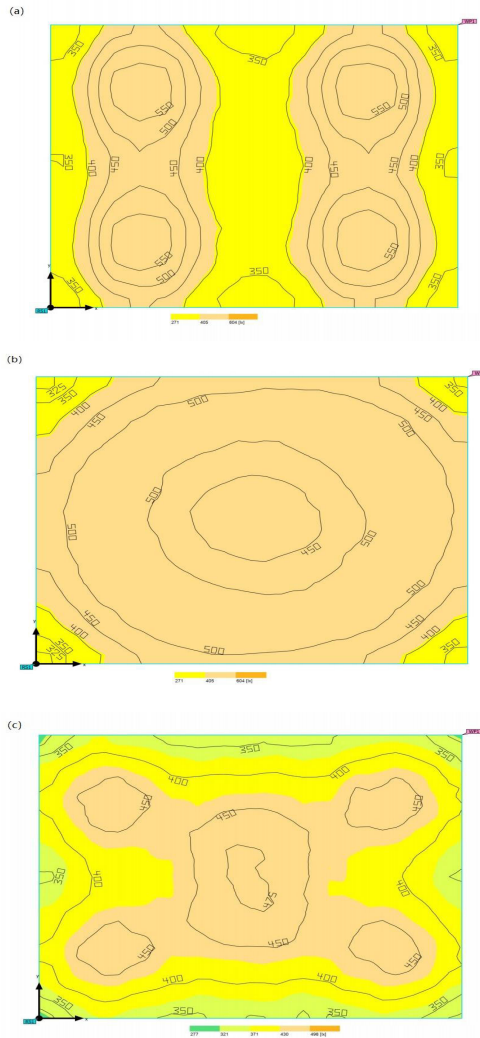


FIGURE 8. (a) Isoillumination map of square layout (b) Isoillumination map of elliptical layout (c) Isoillumination map of square + elliptical layout.

Figure 9(c) is the square + elliptical layout to receive a planar signal-to-noise ratio distribution image. The signal-to-noise ratio ranges from 18.54 to 20.75 dB, and the mean square error is 0.39 dB.

It can be seen from the above that the new layout proposed in this article reduces the number of LEDs by 38, while reducing the fluctuation range of the signal-to-noise ratio, inter-symbol interference, system power consumption, and improving system reliability.

C. ALGORITHM COMPARISON ANALYSIS

Figure 10 is the iterative diagram of the particle swarm algorithm and the adaptive weight simulated annealing particle swarm algorithm proposed in this paper. It is worth nothing from the figure that the particle swarm algorithm reduces the fitness value to about 21 after about 10 iterations, but in the subsequent iteration process, it falls into the local optimal solution and cannot get to the global optimal solution.

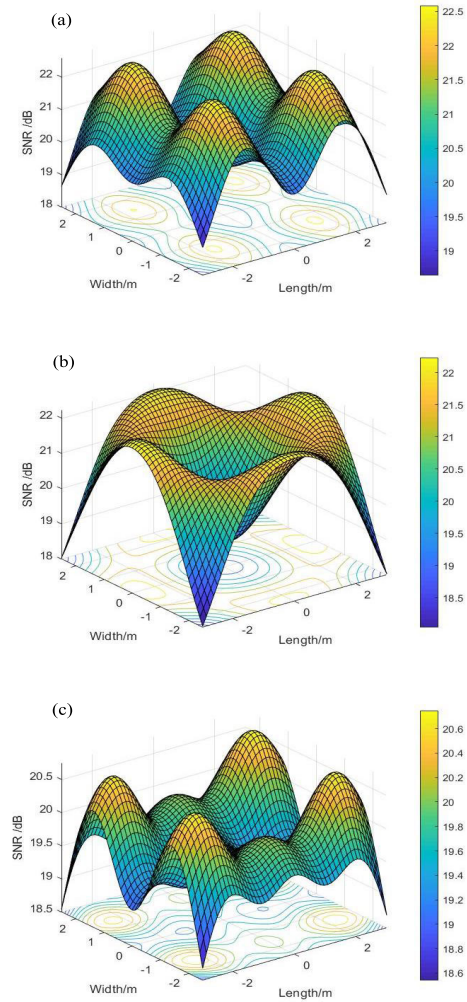


FIGURE 9. (a) SNR distribution of square layout (b) SNR distribution of elliptical layout (c) SNR distribution of square + elliptical layout.

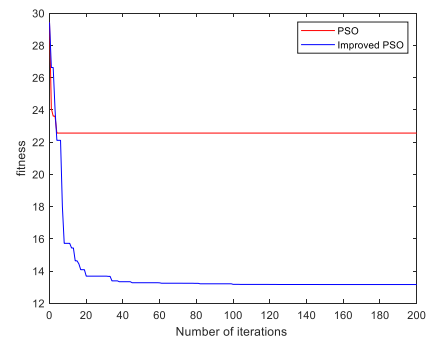


FIGURE 10. Comparison of fitness functions before and after the algorithm is improved.

In contrast, the algorithm proposed in this paper finally finds the global optimal solution after multiple iterations. So it is evident that the improved algorithm can meet the requirements and help to obtain the optimal light source layout.

## V. CONCLUSION

Aiming at the problem of uneven illuminance distribution in visible light communication systems, this paper proposes a square + elliptical layout to build a  $6\text{ m} \times 5\text{ m} \times 3\text{ m}$  room model.

In terms of solving the optimal position, this paper uses the PSO algorithm to advance the process. Because the PSO algorithm has the problem of falling into the local optimal solution, the algorithm is improved from two aspects, and the combination of the mean square error of illuminance and the mean value of the signal-to-noise ratio is set as the fitness function. The optimal light source layout is found. The experimental results indicate that the optimized system illumination range is 359.25 - 451.05 lx, and the mean square error reaches 12.66 lx. The signal-to-noise ratio ranges from 18.54 to 20.75 dB, and the mean square error is 0.39 dB. Compared with the traditional square layout and elliptical layout, while reducing 38 LED light sources, the uniformity of illumination and signal-to-noise ratio is optimized, which provides a new reference solution for the layout of indoor light sources.

## REFERENCES

- [1] K. Lee, H. Park, and J. R. Barry, "Indoor channel characteristics for visible light communications," *IEEE Commun. Lett.*, vol. 15, no. 2, pp. 217–219, Jan. 2011.
- [2] C.-H. Yeh, Y.-L. Liu, and C.-W. Chow, "Real-time white-light phosphor-LED visible light communication (VLC) with compact size," *Opt. Exp.*, vol. 21, pp. 26192–26197, Nov. 2013.
- [3] S. Ragagopai, R. D. Roberts, and S. K. Lim, "IEEE 802.15.7 visible light communication: Modulation schemes and dimming support," *IEEE Commun. Mag.*, vol. 50, no. 3, pp. 77–82, Mar. 2012.
- [4] J. Wang, Z. Su, Z. Yuan, and Y. Zhu, "Study on uniformity of LED array illumination distribution on target plane," *Acta Photonica Sinica*, vol. 43, no. 8, pp. 16–22, 2011.
- [5] Y. C. Jin, X. B. Chen, and X. R. Mao, "Influence of modulation degree on performances of visible light communication system," *Chin. J. Lasers*, vol. 46, no. 5, pp. 380–384, 2019.
- [6] J. Grubor, S. Randel, K.-D. Langer, and J. W. Walewski, "Broadband information broadcasting using LED-based interior lighting," *IEEE J. Lightw. Technol.*, vol. 26, no. 24, pp. 3883–3892, Dec. 15, 2009.
- [7] T. Komine and M. Nakagawa, "Fundamental analysis for visible-light communication system using LED lights," *IEEE Trans. Consum. Electron.*, vol. 50, no. 1, pp. 100–107, Feb. 2004.
- [8] L. Zhao and K. Peng, "Optimization of light source layout in indoor visible light communication based on white light-emitting diode," *Acta Optica Sinica*, vol. 37, no. 7, pp. 1–9, 2017.
- [9] H. Liu, X. Wang, Y. Chen, D. Kong, and P. Xia, "Optimization lighting layout based on gene density improved genetic algorithm for indoor visible light communications," *Opt. Commun.*, vol. 347, May 2020, Art. no. 190565.
- [10] Z. Li, Z. Tong, L. Zhigang, and L. Xueying, "An annular light source layout model for both lighting and communication reliability," *Opto Electron. Eng.*, vol. 45, Jul. 2018, Art. no. 170503.
- [11] Z. Liu, Y. E. Nan, M. A. Ling-Ling, W. Qi, L. Xue-Ying, and Z. Jia-Bao, "Hyperspectral band selection based on improved particle swarm optimization algorithm," *Spectroscopy Spectral Anal.*, vol. 41, no. 10, pp. 3194–3199, 2021.
- [12] S. Liangshan, W. Zhen, and L. Changming, "Optimization algorithm of mine ventilation based on SA-IPSO," *J. Syst. Simul.*, vol. 33, p. 0403, Sep. 2021.
- [13] F. Wei, M. L. Yang, X. J. He, and X. B. Chen, "Simultaneous multi-beam forming method for planar array based on improved particle swarm algorithm," *J. Syst. Eng. Electron.*, pp. 1–10, Sep. 2021.
- [14] T. L. Fu, P. Li, and L. Gao, "Improved LSSVM algorithm considering sample outliers," *Chin. J. Sci. Ins.*, vol. 42, no. 42, pp. 180–190, Jul. 2021.
- [15] T. X. Liu, "A multi-objective particle swarm optimization algorithm with diversity control," *J. XIDIAN Univ.*, vol. 48, no. 3, pp. 106–114, Apr. 2021.
- [16] H. L. Liu and Z. Y. Liu, "Coverage uniformity with improved genetic simulated annealing algorithm for indoor visible light communications," *Opt. Commun.*, vol. 48, no. 1, pp. 76–81, Sep. 2017.



**CHE LIU** was born in 1998. He is currently pursuing the master's degree with the Changchun University of Science and Technology. His research interest includes that the light can be positioned indoors.



**YANFENG TANG** received the Ph.D. degree in communication and information system from the Changchun University of Science and Technology, in 2012. He is currently an Associate Professor with the Department of Electronic Information Engineering, Changchun University of Science and Technology. As the Second Completer, he completed two space optical communication projects from "863" Plan and presided over the completion of three provincial and ministerial scientific research projects; as the Second Completer, he won second prize of the 2011 Jilin Province Science and Technology Progress Award; and as the Main Contributor, he won First Prize of the 2014 Jilin Province Technology Invention. His main research interest includes wireless optical communication theory and technology.



**WENJIE YAN** was born in April 1998. He is currently pursuing the master's degree in ultraviolet communication with the Changchun University of Science and Technology.



**YAFANG BAI** is currently pursuing the master's degree in electronics and communication engineering. His main research interest includes image processing.